Synthesis and crystal structure of $Bi_{6.4}Pb_{0.6}P_2O_{15.2}$
A new polymorph in the series $Bi_{6+x}M_{1-x}P_2O_{15+y}$

N. Arumugam[a], V. Lynch[b], H. Steinfink[a],*

[a]Department of Chemical Engineering and Texas Materials Institute, University of Texas at Austin, 1 University Station C0400, Austin, TX 78712, USA
[b]Department of Chemistry and Biochemistry, University of Texas at Austin, Austin, TX 78712, USA

Abstract

$Bi_{6.4}Pb_{0.6}P_2O_{15.2}$ is a polymorph of structures with the general stoichiometry $Bi_{6+x}M_{1-x}P_2O_{15+y}$. However, unlike previously published structures that consist of layers formed by edge sharing OBi_4 tetrahedra bridged by PO_4 and TO_6 (T = transition metal) tetrahedra and octahedra the title compound's structure is more complex. It is monoclinic, $C2$, $a = 19.4698(4)$ Å, $b = 11.3692(3)$ Å, $c = 16.3809(5)$ Å, $\beta = 101.167(1)°$, $Z = 10$. Single-crystal X-ray diffraction data were refined by least squares on F^2 converging to $R_1 = 0.0387$, $wR_2 = 0.0836$ for 7023 intensities. The crystal twins by mirror reflection across (001) as the twin plane and twin component 1 equals 0.74(1). Oxygen ions are in tetrahedral coordination to four metal ions and the $O(BiPb)_4$ units share corners to form layers that are part of the three-dimensional framework. Eight oxygen ions form a cube around the two crystallographically independent Pb ions. Pb–O bond lengths vary from 2.265(14) to 2.869(14) Å. Pairs of such cubes share an edge to form a Pb_3O_{20} unit. The two oxygen ions from the unshared edges are part of irregular Bi polyhedra. Other oxygen ions of Bi polyhedra are part only of $O(BiPb)_4$ units, and some oxygen ions of the polyhedra are also part of PO_4 tetrahedra. One, two, three and or four PO_4 moieties are connected to the Bi polyhedra. Bi–O bond lengths $\leqslant 3.1$ Å vary from 2.090(12) to 3.07(3) Å. The articulations of Pb cubes, Bi polyhedra and PO_4 tetrahedra link into the three-dimensional structure.
© 2007 Elsevier Inc. All rights reserved.

Keywords: Crystal structure of $Bi_{6.4}Pb_{0.6}P_2O_{15.2}$; Bismuth lead phosphate

1. Introduction

Significant oxygen ion conductivity in a high-temperature polymorph of $Bi_4V_2O_{11}$ [1] has led to intensive investigations of the crystal chemistry and physical properties of compounds synthesized in ternary and quaternary systems Bi–Pb—transition metal—P, V, As–O giving rise to complex phosphates, vanadates and arsenates [2–18]. This search for improved oxygen ion conductors has resulted in important contributions to the understanding of the interrelationship between crystal structure and ion conductivity [16,18]. Many of the structures are related to the high-temperature δ-Bi_2O_3 and CaF_2 motifs that exhibit ion transport properties. Lee et al. [19] synthesized and investigated the ionic conductivity of $PbBi_6M_2O_{15}$ (M = V, P, As) and solid solutions of

$SrBi_6V_2O_{15}$ but did not determine the crystal structure. We have described the syntheses and crystal structures of a new series of compounds $Bi_6TP_2O_{15+x}$, T = 1st row transition metals [20–22] and as part of this investigation also grew single crystals of $Bi_6PbP_2O_{15}$ in anticipation that it might be isostructural with compounds of that series. The X-ray diffraction powder pattern of this phase, however, differed from those in this series but matched the X-ray diffraction powder pattern published by Lee et al. [19]. It became evident that it is a polymorph with a new crystal structure and this determination is reported here.

2. Experimental

2.1. Synthesis

Nominal $Bi_6PbP_2O_{15}$ was synthesized by the solid-state reactions of bismuth trioxide (Bi_2O_3), ammonium dihydrogen

---

*Corresponding author. Fax: +1 512 471 7060.
E-mail address: steinfink@che.utexas.edu (H. Steinfink).

phosphate ($NH_4H_2PO_4$) and lead oxide (PbO). The reactant mixtures were mixed in the ratio of 3:2:1. Prior to their use, Bi_2O_3 was dried in air at 600 °C for 24 h. The mixture was initially heated in air at 195 °C for 5 h to decompose $NH_4H_2PO_4$ and finally at 600 °C for 12 h at a rate of 120 °C/h. The intermediate product was then ground and reheated in air at 800 °C for 10 h and cooled to RT at the rate of 150 °C/h. This product was refired at a higher temperature to ensure the completion of the reaction. The melting point of the sample determined by DTA was 900 ± 5 °C. Single crystals of nominal $Bi_6PbP_2O_{15}$ were obtained by melting a small amount of the polycrystalline sample and slow cooling in a gold boat. $Bi_6PbP_2O_{15}$ melts congruently at 900 ± 5. The temperature of the polycrystalline sample was then raised to 925 °C using a special temperature regime and the melt was kept for 2 h. The melt was slowly cooled at a rate of 5 °C/h to 850 °C, and then furnace cooled to room temperature. Examination of the melt under a polarizing binocular microscope revealed the presence of pale yellow–green crystals. A polycrystalline sample was analyzed by inductively coupled plasma (ICP) optical emission spectroscopy yielding the Bi:Pb ratio 6.8:0.2 on the basis of $P = 2$.

2.2. Crystallography

Single-crystal X-ray diffraction data were obtained using a Nonius κ automated CCD diffractometer equipped with a graphite monochromator with Mo$K\alpha$ radiation,

Table 1
Crystal data and structure refinement for $Bi_{6.40}Pb_{0.60}P_2O_{15.20}$

Empirical formula	$Bi_{6.40}Pb_{0.60}P_2O_{15.20}$
Formula weight	1766.93
Temperature (K)	293(2)
Wavelength (Å)	0.71073
Crystal system, space group	C2
Unit cell dimensions (Å)	
a	19.4698(4)
b	11.3692(3)
c	16.3809(5)
β	101.1674(11)°
Volume (Å^3)	3557.35(16)
Z, calculated density (g/cm)	10, 8.25
Absorption coefficient (mm^{-1})	86.24
Crystal size (mm)	0.08 × 0.05 × 0.02
Crystal color	Yellowish
Theta range for data collection	1.00–27.48°
Limiting indices	$-25 \leqslant h \leqslant 25$, $-14 \leqslant k \leqslant 14$, $-21 \leqslant l \leqslant 21$
Reflections collected/unique	7023/7023 [R(int) = 0.0000]
Completeness to theta (%)	99.9
Absorption correction	SADABS
Refinement method	Full-matrix least-squares on F^2
Data/restraints/parameters	7023/1/339
Goodness-of-fit on F^2	1.046
Final R indices [$I > 2$sigma(I)]	$R_1 = 0.0387$, w$R_2 = 0.0836$
R indices (all data)	$R_1 = 0.0387$, w$R_2 = 0.0836$
Extinction coefficient	0.000146(4)
Largest diff. peak and hole (e Å^{-3})	5.492 and −5.568

Table 2
Atomic coordinates ($\times 10^4$) and equivalent isotropic displacement parameters ($A^2 \times 10^3$) for $Bi_{6.40}Pb_{0.60}P_2O_{15.20}$

Atom	x	y	z	U(eq)[a]
Bi(1)	10000	121(1)	10000	13(1)
Bi(2)	8818(1)	1664(1)	8033(1)	10(1)
Bi(3)	8371(1)	−1635(1)	10035(1)	11(1)
Bi(4)	9398(1)	6346(1)	12049(1)	13(1)
Bi(5)	8921(1)	−1832(1)	8096(1)	13(1)
Bi(6)	8400(1)	5080(1)	10283(1)	17(1)
Bi(7)	7330(1)	6656(1)	8261(1)	8(1)
Bi(8)	7197(1)	3373(1)	7919(1)	9(1)
Bi(9)	7698(1)	−6288(1)	5984(1)	9(1)
Bi(10)	6244(1)	−1378(1)	5932(1)	7(1)
Bi(11)	4486(1)	222(1)	5980(1)	7(1)
Bi(12)	9579(1)	−1450(1)	6008(1)	8(1)
Bi(13)	7999(1)	−3048(1)	6100(1)	11(1)
Bi(14)	6206(1)	−4588(1)	6074(1)	8(1)
Bi(15)	7905(1)	309(1)	5973(1)	8(1)
Bi(16)	10000	3421(1)	10000	20(1)
Bi(17)	10476(1)	3172(1)	7889(1)	13(1)
Pb(1)	10000	6740(1)	10000	21(1)
Pb(2)	8866(1)	4909(1)	8136(1)	15(1)
P(1)	9444(3)	1967(5)	6001(3)	7(1)
P(2)	10498(3)	−256(5)	8012(4)	9(1)
P(3)	7172(3)	−214(5)	7908(4)	10(1)
P(4)	6199(3)	−8021(5)	5854(3)	7(1)
P(5)	6620(2)	6859(5)	10077(3)	9(1)
O(1)	10048(7)	−1200(13)	7401(10)	19(3)
O(2)	7788(6)	4910(11)	8542(8)	8(3)
O(3)	9242(6)	4904(11)	9534(9)	12(3)
O(4)	9317(6)	−5261(11)	11282(8)	10(3)
O(5)	6125(8)	7609(14)	9456(10)	25(4)
O(6)	7931(6)	220(10)	4666(8)	7(3)
O(7)	9630(6)	−3270(11)	8422(8)	8(2)
O(8)	8129(6)	−3087(12)	7404(8)	11(3)
O(9)	9224(6)	6900(12)	6419(8)	13(3)
O(10)	6956(6)	854(11)	8369(8)	9(3)
O(11)	6535(8)	−711(13)	7293(10)	24(3)
O(12)	7395(9)	−1142(16)	8569(12)	37(4)
O(13)	11062(12)	−980(20)	8576(17)	73(7)
O(14)	9300(9)	797(15)	5584(11)	32(4)
O(15)	7887(6)	−401(11)	3117(8)	11(3)
O(16)	10200(10)	2260(18)	6118(14)	50(5)
O(17)	10032(12)	300(20)	8542(15)	59(6)
O(18)	7774(8)	37(14)	7470(11)	25(4)
O(19)	8949(7)	2897(13)	5469(10)	22(3)
O(20)	6300(8)	5665(14)	10260(11)	27(4)
O(21)	10842(12)	540(20)	7512(15)	58(6)
O(22)	7294(8)	6635(15)	9738(11)	32(4)
O(23)	8234(8)	12570(15)	9101(11)	32(4)
O(24)	9236(13)	1840(20)	6847(17)	82(8)
O(25)	6160(7)	−6873(13)	5333(10)	21(3)
O(26)	6750(9)	−7828(16)	6640(12)	42(5)
O(27)	5492(9)	−8352(16)	6014(12)	40(4)
O(28)	6485(8)	−9014(15)	5345(11)	30(4)
O(29)	9327(7)	−1410(13)	9607(10)	20(3)
O(30)	9948(6)	4784(11)	7225(8)	9(3)
O(31)	7245(6)	−1158(11)	5649(8)	8(3)
O(32)	6692(6)	−2976(11)	6418(8)	9(3)
O(33)	8475(6)	−4984(11)	6356(9)	10(3)
O(34)	9541(6)	3101(11)	8436(9)	13(3)
O(35)	8602(6)	−1101(11)	6369(8)	7(3)
O(36)	8150(6)	3069(11)	7473(9)	11(3)
O(37)	8908(7)	6791(12)	10622(9)	14(3)
O(38)	8330(7)	−2863(13)	8972(10)	25(3)

[a] U(eq) is defined as one-third of the trace of the orthogonalized U_{ij} tensor.

$\lambda = 0.71073 \, \text{Å}$. The diffracted intensities generated by a scan of $2.0°$ ω and $340 \, \text{s}$ exposure time per frame were recorded on 93 frames at $\phi = 186°$, 58 frames over a range of $116°$ ω, and 55 frames over a range of $110°$ ω. The intensities were collected on the basis of a C-centered monoclinic cell, $a = 19.4500(3) \, \text{Å}$, $b = 11.3388(2) \, \text{Å}$, $c = 16.3379(3) \, \text{Å}$, $\beta = 101.0773(6)°$. Data reduction and scaling were performed using DENZO-SMN [23]. Details of crystal data, data collection and structure refinement are

listed in Table 1. The structure was solved with the direct methods program SHELXS [24] in space group $C2$ that yielded the heavy atom positions. Difference electron density maps revealed the phosphorus and oxygen atoms. The refinement proceeded by least squares using SHELXL [24], DENZO-style merged intensities, anisotropic displacement parameters for Bi and Pb, eventually converging to $R_1 = 0.0494$ and Flack x parameter 0.24. The program ROTAX [25] indicated that the crystal was a
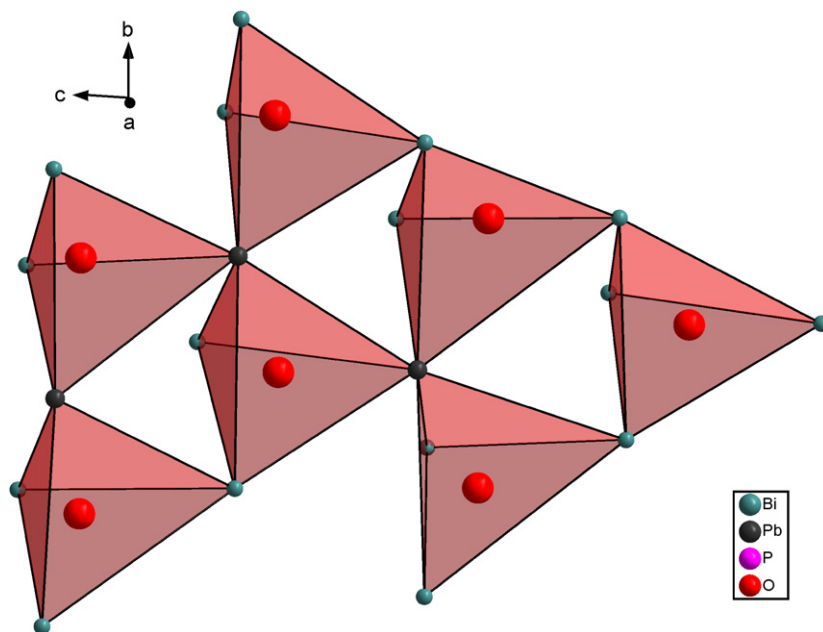

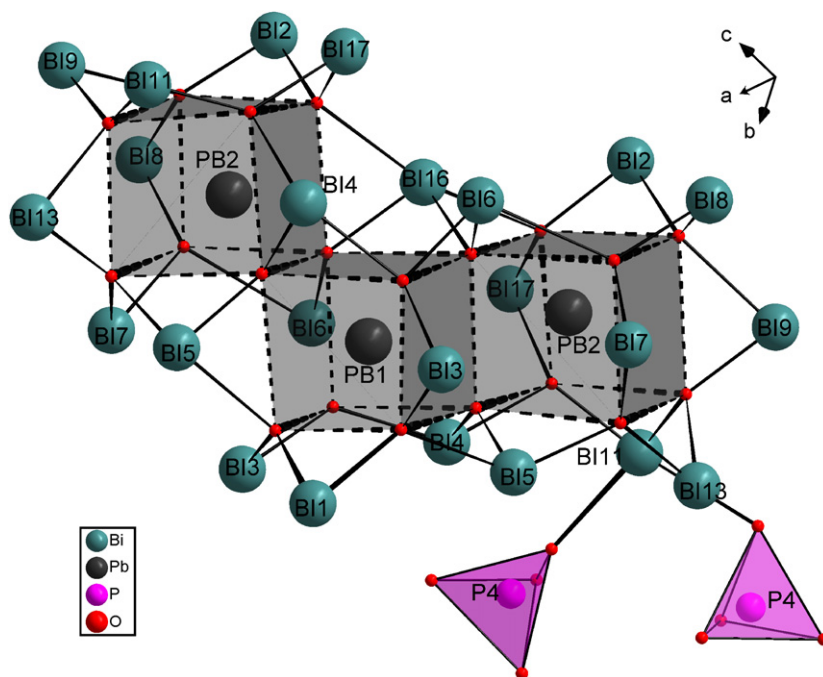Fig. 1. Section of the crystal structure of $Bi_{6.4}Pb_{0.6}P_2O_{15.2}$ showing the corner sharing oxygen tetrahedra $O(BiPb)_4$ in the b–c plane.

Fig. 2. Section of the crystal structure of $Bi_{6.4}Pb_{0.6}P_2O_{15.2}$ showing the articulation of the cubic Pb polyhedra, the bonding of unshared oxygen edges to Bi and illustrating the connection of two PO_4 tetrahedra to Bi.
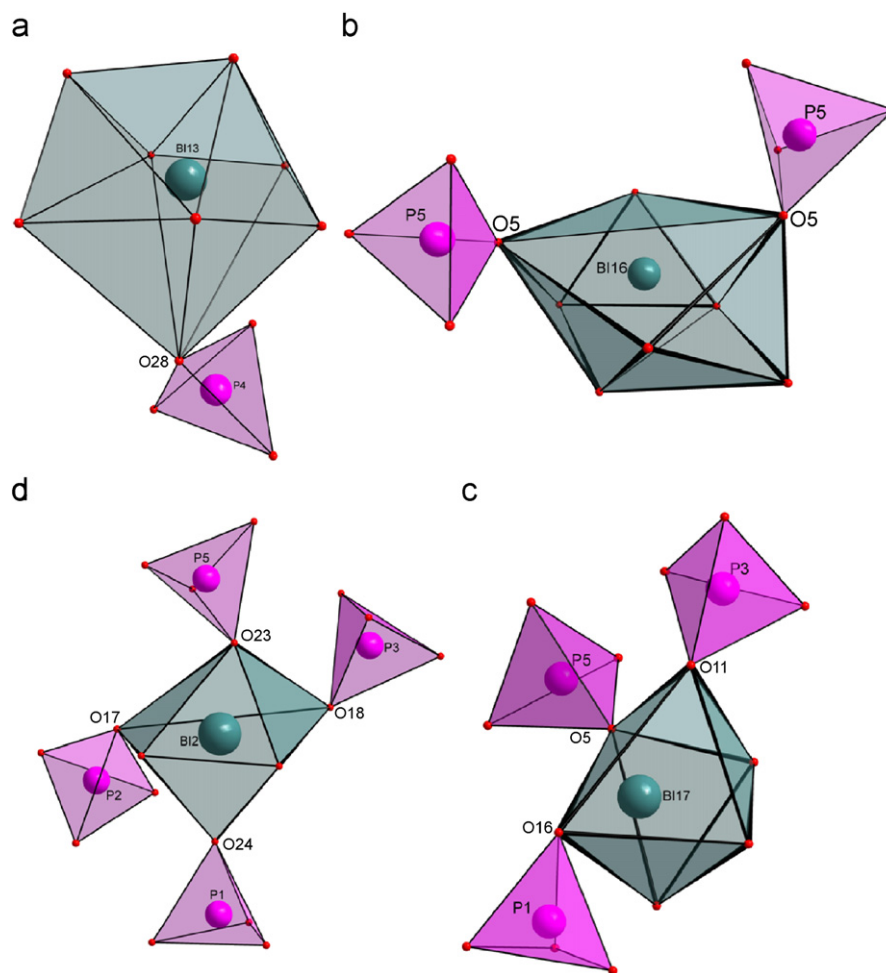
Fig. 3. Selected Bi–O polyhedra and bonding to (a) one, (b) two, (c) three and (d) four PO_4 moieties.
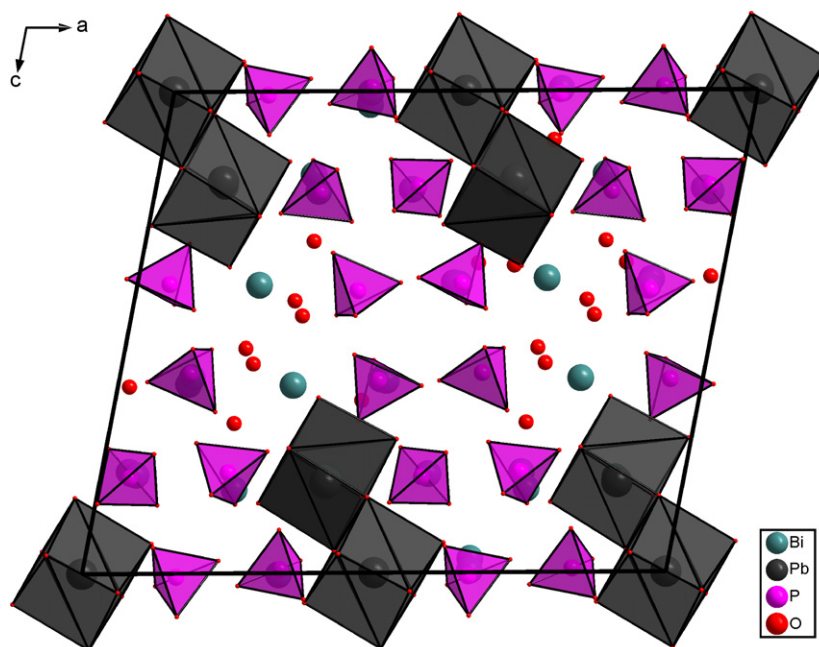

Fig. 4. The crystal structure of $Bi_{6.4}Pb_{0.6}P_2O_{15.2}$ looking parallel to the *b*-axis. For the sake of clarity only the Pb and P polyhedra are shown. Bonds among Bi and oxygen ions are omitted.

Table 3
Bond lengths (Å), valence bond sums (VBS) and angles (deg) for $Bi_{6.4}Pb_{0.6}P2O_{15.2}$

Bi(1)–O(29)	2.199(15)	Bi(2)–O(36)	2.151(13)	Bi(3)–O(29)	2.126(13)	Bi(4)–O(4)#5	2.206(13)	Bi(5)–O(7)	2.141(12)
Bi(1)–O(29)#1	2.199(15)	Bi(2)–O(34)	2.175(13)	Bi(3)–O(37)#4	2.198(14)	Bi(4)–O(7)#6	2.220(11)	Bi(5)–O(8)	2.240(13)
Bi(1)–O(17)#1	2.41(2)	Bi(2)–O(24)	2.26(3)	Bi(3)–O(38)	2.220(16)	Bi(4)–O(30)#1	2.366(12)	Bi(5)–O(38)	2.323(15)
Bi(1)–O(17)	2.41(2)	Bi(2)–O(23)#4	2.488(16)	Bi(3)–O(13)#1	2.44(3)	Bi(4)–O(37)	2.402(14)	Bi(5)–O(29)	2.496(16)
Bi(1)–O(20)#2	2.560(15)	Bi(2)–O(18)	2.770(16)	Bi(3)–O(20)#3	2.757(16)	Bi(4)–O(10)#7	2.653(12)	Bi(5)–O(1)	2.756(13)
Bi(1)–O(20)#3	2.560(15)	Bi(2)–O(17)	2.82(2)	Bi(3)–O(12)	2.816(18)	Bi(4)–O(1)#6	3.063(15)	Bi(5)–O(35)	2.897(13)
		Bi(2)–O(20)#3	3.068(16)	Bi(3)–O(22)#4	2.848(16)			Bi(5)–O(18)	3.108(16)
VBS 2.93		VBS 3.02		VBS 3.22		VBS 2.83		VBS 2.90	
Bi(6)–O(37)	2.203(14)	Bi(7)–O(38)#5	2.138(15)	Bi(8)–O(36)	2.150(12)	Bi(9)–O(33)	2.121(13)	Bi(10)–O(32)	2.103(12)
Bi(6)–O(4)#5	2.210(13)	Bi(7)–O(2)	2.189(12)	Bi(8)–O(15)#10	2.178(13)	Bi(9)–O(6)#11	2.251(12)	Bi(10)–O(31)	2.104(11)
Bi(6)–O(3)	2.238(12)	Bi(7)–O(8)#5	2.306(12)	Bi(8)–O(2)	2.229(13)	Bi(9)–O(15)#11	2.266(12)	Bi(10)–O(11)	2.318(16)
Bi(6)–O(10)#7	2.594(13)	Bi(7)–O(22)	2.435(17)	Bi(8)–O(26)#5	2.511(19)	Bi(9)–O(36)#4	2.534(14)	Bi(10)–O(19)#11	2.399(16)
Bi(6)–O(22)	2.796(16)	Bi(7)–O(12)#5	2.552(18)	Bi(8)–O(23)#4	2.672(18)	Bi(9)–O(31)#11	2.703(13)	Bi(10)–O(16)#12	2.62(2)
Bi(6)–O(2)	2.876(14)	Bi(7)–O(32)#5	3.063(13)	Bi(8)–O(13)#9	2.74(2)	Bi(9)–O(19)#4	2.881(14)	Bi(10)–O(28)#5	2.923(16)
Bi(6)–O(5)#3	2.962(15)			Bi(8)–O(10)	3.016(12)	Bi(9)–O(26)	2.898(18)		
Bi(6)–O(12)#7	2.999(17)					Bi(9)–O(25)	3.052(14)		
VBS 2.95		VBS 3.09		VBS 3.14		VBS 3.02		VBS 3.28	
Bi(11)–O(30)#12	2.123(13)	Bi(12)–O(35)	2.135(11)	Bi(13)–O(8)	2.102(13)	Bi(14)–O(32)	2.090(12)	Bi(15)–O(31)	2.109(12)
Bi(11)–O(9)#12	2.136(13)	Bi(12)–O(9)#4	2.152(13)	Bi(13)–O(9)#4	2.342(12)	Bi(14)–O(15)#11	2.198(13)	Bi(15)–O(35)	2.120(12)
Bi(11)–O(33)#9	2.186(12)	Bi(12)–O(1)	2.305(16)	Bi(13)–O(33)	2.393(13)	Bi(14)–O(6)#11	2.265(12)	Bi(15)–O(6)	2.155(13)
Bi(11)–O(27)#5	2.536(18)	Bi(12)–O(25)#10	2.430(16)	Bi(13)–O(35)	2.505(12)	Bi(14)–O(21)#12	2.59(2)	Bi(15)–O(18)	2.532(16)
Bi(11)–O(28)#14	2.729(17)	Bi(12)–O(14)	2.675(17)	Bi(13)–O(31)	2.627(12)	Bi(14)–O(14)#11	2.737(18)	Bi(15)–O(28)#5	2.861(16)
Bi(11)–O(19)#12	2.905(15)	Bi(12)–O(27)#15	2.799(17)	Bi(13)–O(32)	2.695(12)	Bi(14)–O(25)	2.862(15)	Bi(15)–O(14)	2.961(16)
				Bi(13)–O(6)#11	2.802(12)	Bi(14)–O(16)#12	2.88(2)		
				Bi(13)–O(28)#10	2.956(16)				
VBS 3.19		VBS 3.10		VBS 2.98		VBS 3.08		VBS 3.34	
Bi(16)–O(3)#1	2.273(13)	Bi(17)–O(34)	2.181(12)	Pb(1)–O(29)#6	2.496(15)	Pb(2)–O(3)	2.265(14)		
Bi(16)–O(3)	2.273(13)	Bi(17)–O(4)#6	2.229(13)	Pb(1)–O(29)#5	2.496(15)	Pb(2)–O(2)	2.321(11)		
Bi(16)–O(34)	2.571(15)	Bi(17)–O(30)	2.273(13)	Pb(1)–O(37)#1	2.530(13)	Pb(2)–O(34)	2.437(13)		
Bi(16)–O(34)#1	2.571(15)	Bi(17)–O(5)#2	2.708(17)	Pb(1)–O(37)	2.530(13)	Pb(2)–O(7)#5	2.540(12)		
Bi(16)–O(5)#2	2.683(15)	Bi(17)–O(11)#15	2.757(14)	Pb(1)–O(7)#5	2.545(13)	Pb(2)–O(36)	2.630(13)		
Bi(16)–O(5)#3	2.683(15)	Bi(17)–O(16)	3.03(2)	Pb(1)–O(7)#6	2.545(13)	Pb(2)–O(30)	2.810(11)		
Bi(16)–O(4)#6	3.083(12)	Bi(17)–O(24)	3.07(3)	Pb(1)–O(3)	2.585(13)	Pb(2)–O(8)#5	2.832(13)		
Bi(16)–O(4)#5	3.083(12)			Pb(1)–O(3)#1	2.585(13)	Pb(2)–O(33)#5	2.869(14)		
VBS 2.33		VBS 2.67		VBS 2.59		VBS 2.74			
P(1)–O(16)	1.48(2)	P(2)–O(21)	1.47(2)	P(3)–O(12)	1.514(19)	P(4)–O(27)	1.497(17)	P(5)–O(5)	1.521(17)
P(1)–O(14)	1.497(18)	P(2)–O(17)	1.51(2)	P(3)–O(18)	1.515(15)	P(4)–O(26)	1.52(2)	P(5)–O(22)	1.541(16)
P(1)–O(24)	1.52(3)	P(2)–O(13)	1.53(3)	P(3)–O(10)	1.532(13)	P(4)–O(25)	1.552(16)	P(5)–O(20)	1.547(17)
P(1)–O(19)	1.576(16)	P(2)–O(1)	1.607(16)	P(3)–O(11)	1.545(16)	P(4)–O(28)	1.569(17)	P(5)–O(23)#3	1.549(19)
O(16)–P(1)–O(14)	110.6(11)	O(21)–P(2)–O(17)	116.9(13)	O(12)–P(3)–O(18)	109.2(9)	O(27)–P(4)–O(26)	114.1(10)	O(5)–P(5)–O(22)	109.0(9)
O(16)–P(1)–O(24)	109.6(13)	O(21)–P(2)–O(13)	108.6(13)	O(12)–P(3)–O(10)	105.5(9)	O(27)–P(4)–O(25)	111.1(9)	O(5)–P(5)–O(20)	113.2(9)
O(14)–P(1)–O(24)	105.7(13)	O(17)–P(2)–O(13)	108.5(14)	O(18)–P(3)–O(10)	113.3(8)	O(26)–P(4)–O(25)	107.1(10)	O(22)–P(5)–O(20)	109.1(9)
O(16)–P(1)–O(19)	113.9(10)	O(21)–P(2)–O(1)	108.6(11)	O(12)–P(3)–O(11)	107.1(9)	O(27)–P(4)–O(28)	110.2(10)	O(5)–P(5)–O(23)#3	106.0(10)
O(14)–P(1)–O(19)	107.6(10)	O(17)–P(2)–O(1)	108.7(11)	O(18)–P(3)–O(11)	111.0(9)	O(26)–P(4)–O(28)	106.7(10)	O(22)–P(5)–O(23)#3	112.0(9)
O(24)–P(1)–O(19)	108.9(12)	O(13)–P(2)–O(1)	104.9(12)	O(10)–P(3)–O(11)	110.4(8)	O(25)–P(4)–O(28)	107.3(8)	O(20)–P(5)–O(23)#3	107.6(9)

Symmetry transformations used to generate equivalent atoms: #1: $-x+2, y, -z+2$; #2: $x+1/2, y-1/2, z$; #3: $-x+3/2, y-1/2, -z+2$; #4: $x, y-1, z$; #5: $x, y+1, z$; #6: $-x+2, y+1, -z+2$; #7: $-x+3/2, y+1/2, -z+2$; #8: $-x+3/2, y+3/2, -z+2$; #9: $x-1/2, y+1/2, z$; #10: $-x+3/2, y+1/2, -z+1$; #11: $-x+3/2, y-1/2, -z+1$; #12: $x-1/2, y-1/2, z$; #13: $-x+1, y, -z+1$; #14: $-x+1, y+1, -z+1$; #15: $x+1/2, y+1/2, z$; #16: $-x+2, y-1, -z+2$; #17: $-x+3/2, y-3/2, -z+2$; #18: $x+1/2, y+3/2, z$; #19: $-x+3/2, y+3/2, -z+1$; #20: $-x+2, y, -z+1$; #21: $-x+3/2, y-3/2, -z+1$; #22: $x-1/2, y-3/2, z$; #23: $-x+1, y-1, -z+1$.

twin with (0 0 1) as the twin plane having a twin component 1 equal to 0.74(1). Including twinning in the refinement yielded $R_1 = 0.0488$. The resultant stoichiometry was $Bi_{6.4}Pb_{0.6}P_2O_{15.2}$. The ICP derived data were high in Bi content even though the X-ray diffraction powder pattern appeared to be single phase. Absorption corrected intensities using the program SADABS [26] with the same refinement conditions converged to $R_1 = 0.0387$. The final atomic parameters are shown in Table 2. Since X-ray scattering cannot distinguish between Pb and Bi, valence bond sum calculations [27] and crystal chemical considerations were used for the atom assignment.

3. Results and discussion

The crystal architecture is complex and is best described by selected fragments. The motif is consistent with that of previously published structures. Oxygen ions are in

tetrahedral coordination to four metal ions and the $O(BiPb)_4$ units share corners to form part of the three-dimensional framework (Fig. 1). Pb1 and Pb2 ions are in cubic coordination to oxygen and share one edge to form a trimer Pb_3O_{20}. The two oxygen ions from the unshared edges are part of Bi polyhedra (Fig. 2). Some of the oxygen ions of Bi polyhedra are also part of PO_4 tetrahedra while other oxygen ions of Bi polyhedra are part only of $O(BiPb)_4$ units. Selected Bi–O polyhedra and their bonding to one, two, three and four PO_4 moieties are shown in Fig. 3. The articulations of Pb cubes, Bi polyhedra and PO_4 tetrahedra link into the three-dimensional structure as shown in Fig. 4.

In Table 3 are listed bond lengths and valence bond sums for Bi–O, Pb–O and pertinent parameters for the PO_4 tetrahedra. As expected the coordination polyhedra around Bi are distorted due to the presence of the non-binding $6s^2$ electrons. The polyhedra vary from distorted octahedra, Bi1, Bi2, Bi4, Bi10 and Bi12 to monocapped, bicapped and tricapped octahedra Bi5, Bi8, Bi9, Bi14, Bi15 and Bi17, capped rectangular pyramids Bi6, Bi11, mono-capped distorted trigonal prism Bi3, monocapped penta-gonal prism Bi13 and a distorted square antiprism Bi16. The polyhedral description around Bi is somewhat arbitrary because of the irregular arrangements of oxygen forced by the presence of the $6s^2$ electrons and the cut off of bonds at $\leqslant 3.11$ Å. The articulations of these tetrahdra and polyhedra are shown in Fig. 4 and provide rigidity to the three-dimensional framework.

4. Conclusion

The relatively low reported conductivities of 10^{-5} to 10^{-7} S/cm at 500 °C for these materials [19] can be ascribed to the rigid structure formed by the articulation of cubic, tetrahedral and irregular polyhedra. The introduction of defects, e.g. vacancies and aliovalent substitutions improve anion transport [16,18].

Supplementary materials

The crystallographic cif file for $Bi_{6.4}Pb_{0.6}P_2O_{15.2}$ was deposited with FIZ Karlsruhe as CSD number 418094. The data may be obtained without charge from FIZ Karlsruhe; fax: +49 7247 808 666; or e-mail: crysdata@fiz-karlsruhe.de.

Acknowledgments

References

[1] F. Abraham, M.F. Debreuille-Gresse, G. Mairesse, G. Nowogrocki, Solid State Ionics 28–30 (1988) 529.
[2] J.C. Boivin, G. Mairesse, Chem. Mater. 10 (1998) 2870.
[3] J. Huang, A.W. Sleight, J. Solid State Chem. 100 (1992) 170.
[4] J. Huang, Q. Gu, A.W. Sleight, J. Solid State Chem. 105 (1993) 599.
[5] I. Radosavljevic, J.S.O. Evans, A.W. Sleight, J. Solid State Chem. 137 (1998) 143.
[6] I. Radosavljevic, J.S.O. Evans, A.W. Sleight, J. Solid State Chem. 141 (1998) 149.
[7] I. Radosavljevic, J.S.O. Evans, A.W. Sleight, J. Alloys Compds. 284 (1999) 99.
[8] F. Abraham, M. Ketatni, G. Mairesse, B. Mernari, Eur. J. Solid State Chem. 31 (1994) 313.
[9] A. Mizrahi, J.P. Wignacourt, H. Steinfink, J. Solid State Chem. 133 (1997) 516.
[10] S. Giraud, J.P. Wignacourt, M. Drache, G. Nowogrocki, H. Steinfink, J. Solid State Chem. 142 (1999) 80.
[11] A. Mizrahi, J.P. Wignacourt, M. Drache, P. Conflant, J. Mater. Chem. 5 (1995) 901.
[12] M. Ketatni, F. Abraham, O. Mentre, Solid State Sci. 1 (1999) 449.
[13] M. Ketatni, B. Mernari, F. Abraham, O. Mentre, J. Solid State Chem. 153 (2000) 48.
[14] Y.-C. Jie, Heidelberger geowissenschaftliche Abhandlungen 84 (1995) 1.
[15] Y.-C. Jie, W. Wysel, Powder Diffr. 10 (1995) 76.
[16] S. Giraud, S. Obbade, E. Suard, H. Steinfink, J.P. Wignacourt, Solid State Sci. 5 (2003) 335.
[17] F. Abraham, O. Cousin, O. Mentre, El.M. Ketatni, J. Solid State Chem. 167 (2002) 168.
[18] P. Roussel, S. Giraud, E. Suard, J.-P. Wignacourt, H. Steinfink, Solid State Sci. 4 (2002) 1143.
[19] C.K. Lee, C.S. Lee, A. Watanabe, D.C. Sinclair, Solid State Ionics 171 (2004) 237.
[20] H. Steinfink, V. Lynch, J. Solid State Chem. 177 (2004).
[21] R.I. Dass, V. Lynch, R.L. Harlow, H. Steinfink, Mater. Res. Bull. 41 (2006) 1543.
[22] N. Arumugam, V. Lynch, H. Steinfink, J. Solid State Chem. 180 (2007) 1504.
[23] Z. Otwinowski, W. Minor. DENZO-SMN. Methods in enzymology,, in: C.W. Carter Jr., R.M. Sweets (Eds.), Macromolecular Crystallography, Part A, vol. 276, Academic Press, 1997, pp. 307–326.
[24] G. M. Sheldrick, SHELXS 97-2, a program for automatic solution of crystal structures and SHELXL 97-2, a program for crystal structure refinement, University of Göttingen, Germany, 1997 as incorporated in the WINGX program suite L. J. Farrugia, WinGX v. 1.70.01, J. Appl. Cryst. 32 (1999) 837.
[25] ROTAX: Simon Parsons and Bob Gould, University of Edinburgh with additions by Richard Cooper (Oxford) and Louis Farrugia (Glasgow) Version 26th November, 2001 as incorporated in WINGX.
[26] G.M. Sheldrick, SHELXTL Version 6.14 Bruker Analytical X-ray Instruments, Inc. Madison, WI, USA, 2003.
[27] A.S. Wills, I.D. Brown, VALIST 1.0, CEA, France, 1999.